The Journal of Veterinary Medical Science

NOTE

Pathology

Malignant rhabdoid tumor of the musk gland and systemic T-cell lymphoma in a masked palm civet (*Paguma larvata*)

Yukino MACHIDA[1)], Masaki MICHISHITA[1)]*, Hisashi YOSHIMURA[2)], Takuya KATO[3)], Shin-ichi HAYAMA[3)] and Kimimasa TAKAHASHI[1)]

[1)]Department of Veterinary Pathology, School of Veterinary Medicine, Nippon Veterinary and Life Science University, 1-7-1 Kyonan-cho, Musashino, Tokyo 180-8602, Japan

[2)]Division of Physiological Pathology, Department of Applied Science, School of Veterinary Nursing and Technology, Nippon Veterinary and Life Science University, 1-7-1 Kyonan-cho, Musashino, Tokyo 180-8602, Japan

[3)]Department of Wildlife Medicine, School of Veterinary Medicine, Nippon Veterinary and Life Science University, 1-7-1 Kyonan-cho, Musashino, Tokyo 180-8602, Japan

J. Vet. Med. Sci.
81(7): 975–979, 2019
doi: 10.1292/jvms.18-0616

Received: 19 October 2018
Accepted: 7 May 2019
Advanced Epub:
16 May 2019

ABSTRACT. A 21-year-old male masked palm civet died after 2 months of continuous abdominal distention and poor appetite. Grossly, both musk glands were markedly swelled. Microscopically, round, polygonal and spindle neoplastic cells proliferated diffusely in the right musk gland and a metastatic focus was observed in the lung. The neoplastic cells had abundant cytoplasm with faintly eosinophilic inclusions that ultrastructurally corresponded to whorl aggregates of intermediate filaments. Immunohistochemically, these cells were positive for vimentin, cytokeratins and glial fibrillary acidic protein and negative for desmin. Based on these findings, the tumor was diagnosed as malignant rhabdoid tumor. Papillary adenoma was seen in the opposite musk gland. T-cell lymphoma of the lymph nodes, small intestine and liver was considered as the cause of death.

KEY WORDS: lymphoma, malignant rhabdoid tumor, masked palm civet, musk gland

Masked palm civet (*Paguma larvata*), a member of the family Viverridae, inhabits widespread areas of Asia, but it is an alien species in Japan and thought to be have been introduced from Taiwan [15]. In Japan, masked palm civets are known as carriers of human and animal pathogens such as hepatitis E virus, canine distemper virus, *Salmonella enterica*, *Campylobacter* spp. and *Yersinia pseudotuberculosis* [11, 13, 28], which can cause serious public and animal health problems. Viverridae, including the small Indian civet and masked palm civet, possesses musk glands that are located between the anus and genital opening in males and produce a malodorous substance [4]. As for spontaneous tumors in palm civets, pancreatic carcinoma and hepatocellular carcinoma have been reported [20, 26].

In humans, rhabdoid tumor is a rare pediatric neoplasm occurring in the kidneys and it was originally described as a subtype of Wilms' tumor. The tumor is characterized by clinically aggressive behaviors, as represented by metastases to the lymph nodes and poor prognosis [1, 14]. In adults, malignant extrarenal rhabdoid tumors that are histopathologically similar to its renal counterparts have also been reported in various organs, including the soft tissue, brain, liver and colon [14, 17]. Rhabdoid tumors are histopathologically characterized by proliferation of poorly differentiated neoplastic cells showing large and eccentric nuclei, prominent nucleoli, and intracytoplasmic glossy eosinophilic inclusions. The inclusions are immunohistochemically positive for cytokeratin and vimentin, and negative for desmin, neurofilament and S-100, and ultrastructurally correspond to whorl aggregates of intermediate filaments [1, 10, 17]. Therefore, both immunohistochemical and ultrastructural examinations are most necessary to diagnose rhabdoid tumors. In animals, four cases of rhabdoid tumors have so far been reported in the stomach of an orangutan, brain of a dog, skin of a cat and orbit of a horse [8, 10, 21, 23]. To the best of our knowledge, there are no reports describing a malignant rhabdoid tumor arising in the musk glands of masked palm civet. In this report, we describe the histopathological and ultrastructural features of a malignant rhabdoid tumor occurring in the right musk gland, simultaneously accompanied by adenoma in the left musk gland and systemic T-cell lymphoma in a masked palm civet.

A 21-year-old male masked palm civet that was kept indoors as a pet died after 2 months of continuous abdominal distention and poor appetite. No clinical examinations were performed. Tissues collected during necropsy were fixed in 10% neutral buffered

*Correspondence to: Michishita, M.: michishita@nvlu.ac.jp

Table 1. Primary antibodies used in the present case

Antibody	Clone	Dilution	Source	Antigen retrieval	Positive control tissue (masked palm civet)
Cytokeratin	AE1/AE3	1:200	Dako, Glostrup, Denmark	121°C for 10 min in citrate buffer, pH 6.0	Musk gland
Cytokeratin 8	Ks 8.7	1:50	PROGEN, Heidelberg, Germany	121°C for 10 min in citrate buffer, pH 6.0	Musk gland
Vimentin	V9	1:100	Dako	121°C for 10 min in citrate buffer, pH 6.0	Musk gland
Desmin	D33	1:200	Dako	121°C for 10 min in citrate buffer, pH 6.0	Skeletal muscle
αSMA	1A4	1:400	Dako	121°C for 10 min in citrate buffer, pH 6.0	Musk gland
NSE	BBS/NC/VI-H14	1:200	Dako	121°C for 10 min in citrate buffer, pH 6.0	Pancreas
CD204	SRA-E5	1:100	TransGenic, Kumamoto, Japan	Microwave for 10 min in citrate buffer, pH 2.0	Lymph node
Ki-67	MIB-1	1:100	Dako	121°C for 20 min in citrate buffer, pH 6.0	Lymph node
BLA36	A27-42	1:300	BioGenex, Fremont, CA, U.S.A.	121°C for 10 min in citrate buffer, pH 6.0	Lymph node
Neurofilament	2F11	1:200	Dako	121°C for 10 min in citrate buffer, pH 6.0	Peripheral nerve
CD3	Polyclonal	1:300	Dako	121°C for 10 min in citrate buffer, pH 6.0	Lymph node
S-100	Polyclonal	1:1,500	Dako	121°C for 10 min in citrate buffer, pH 6.0	Peripheral nerve
GFAP	Polyclonal	1:800	Dako	121°C for 10 min in citrate buffer, pH 6.0	Musk gland (myoepithelial cell)
vWF	Polyclonal	Prediluted	Nichirei Biosciences Inc., Tokyo, Japan	37°C for 20 min in 0.1% trypsin	Musk gland
Iba-1	Polyclonal	1:1,000	Wako, Osaka, Japan	121°C for 10 min in citrate buffer, pH 6.0	Lymph node
Lysozyme	Polyclonal	1:300	Dako	37°C for 20 min in 0.1% trypsin	Lymph node

formalin, processed routinely and embedded in paraffin wax. Sections (4 μm) were stained with hematoxylin and eosin, periodic acid-Schiff (PAS) and phosphotungstic acid-hematoxylin (PTAH). Serial sections were then subjected to immunohistochemical analysis using primary antibodies listed in Table 1. After reaction with the primary antibodies, the sections were incubated with biotinylated goat anti-mouse immunoglobulin G (IgG) or anti-rabbit IgG antibodies (Dako Japan, Tokyo, Japan), followed by peroxidase-conjugated streptavidin. Finally, the sections were visualized following addition of diaminobenzidine tetrahydrochloride and counterstained with hematoxylin. The antibodies were validated by a positive reaction with the normal musk glands, lymph nodes and brain obtained from a 17-month-old male masked palm civet and by a negative reaction due to replacement of the antibodies with normal mouse or rabbit IgG. For electron microscopic examination, small pieces of the formalin-fixed right musk gland tissue were refixed in 1% osmium tetroxide in 0.2 M phosphate buffer and then embedded in epoxy resin. Ultrathin sections were examined using a JEM-1011 electron microscope (JEOL, Tokyo, Japan) after staining with uranyl acetate and lead citrate.

The right and left musk gland were enlarged up to 4.2 × 3.5 × 2.0 and 3.2 × 2.1 × 1.5 cm, respectively. The cut surfaces were pale red with dark red spots (right) and pale peach in color (left) (Fig. 1). In addition to the enlarged musk glands, the mesenteric and renal lymph nodes were swelled measuring 9.0 × 6.0 × 4.0 cm and 3.8 × 1.7 × 0.9 cm, respectively, and multiple masses, measuring 1.5 to 3.0 cm in diameter, were seen in the liver. Moreover, partial thickening of the ileojejunal wall occurred in the range of 5 cm long. Microscopically, round, polygonal and spindle neoplastic cells proliferated diffusely and infiltrated the surrounding parenchyma in the right musk gland (Fig. 2). They contained hypochromatic nuclei and abundant cytoplasm with faintly eosinophilic inclusions that were negative for PAS and PTAH stains (Fig. 3). Multinucleated giant cells were often observed. The frequency of mitosis in the neoplastic cells was 0–1 per high-power field (400×). The pre-existing glandular cells adjacent to the neoplastic tissue also exhibited papillary and cystic hyperplasia (Fig. 4). A metastatic focus of the neoplastic cells was detected in the lung (Fig. 5). Immunohistochemically, the neoplastic cells were diffusely positive for vimentin, partially positive for cytokeratin (CK) AE1/AE3 (Fig. 6) and CK8, weakly positive for glial fibrillary acidic protein (GFAP) (Fig. 7) and neuron-specific enolase (NSE) and negative for S-100, neurofilament, alpha-smooth muscle actin (αSMA), desmin, p63, lysozyme, CD3, BLA36, HLA-DR, Iba-1, CD204 and von Willebrand factor. Both luminal and myoepithelial cells in the normal musk gland were diffusely positive for CK AE1/AE3, vimentin and αSMA, whereas p63 were expressed in the myoepithelial cells, but not in the luminal cells. Ki-67 index of the rhabdoid cells was 29.2%. The immunohistochemical features of the metastatic tumor in the lung were similar to those of the primary tumor seen in the right musk gland. Ultrastructural analysis showed that the cytoplasm of the neoplastic cells contained whorl aggregates of intermediate filaments, approximately 10 μm diameter, corresponding to faintly eosinophilic inclusions (Fig. 8). Also, papillary adenoma was also observed in the left musk gland.

The enlarged mesenteric and renal lymph nodes and the masses in the liver represented diffuse proliferation of neoplastic lymphoid cells. In the ileojejunum, neoplastic lymphoid cells proliferated diffusely in the mucosal lamina propria and submucosa (Fig. 9). The neoplastic cells had a large hypochromatic nucleus with large nucleoli and scarce cytoplasm (Fig. 10). The frequency of mitosis was 0−2 per high-power field. These cells were diffusely positive for CD3 (Fig. 11), and negative for BLA36. Besides these neoplasms, some spontaneous lesions such as pulmonary edema, early fibrosis and hepatocellular hyperplasia in the liver, and calculus and tubular cysts in the kidney were noted.

On the basis of these anatomical, morphological, immunohistochemical and ultrastructural findings, we arrived at a diagnosis of malignant rhabdoid tumor arising from the right musk gland, adenoma in the left musk gland, and systemic T-cell lymphoma.

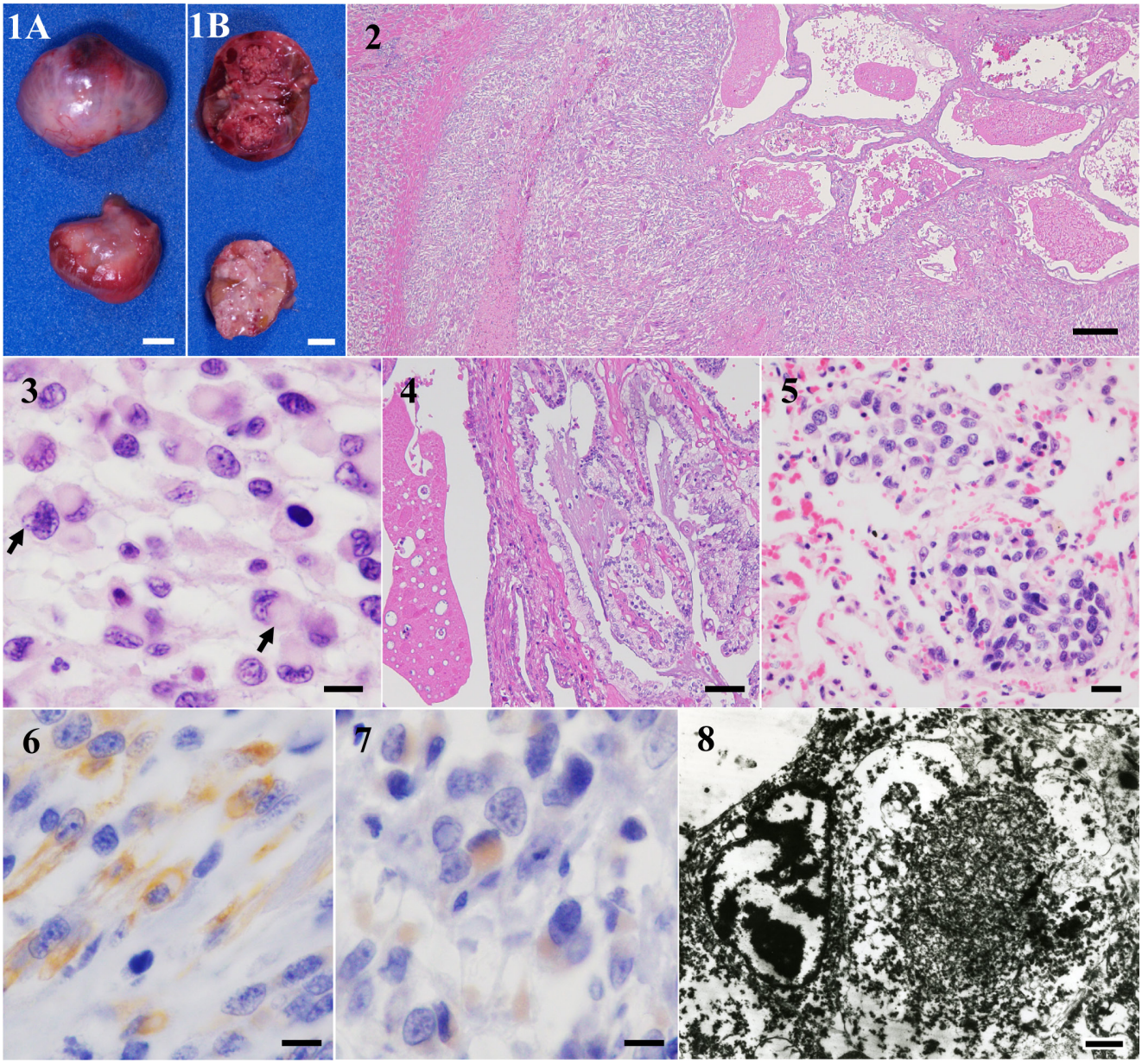

Fig. 1. Gross appearance of the musk glands in a masked palm civet. A, the enlarged musk glands (upper, right; bottom, left). B, cut surface of the musk glands (upper, right; bottom, left). Bar=1 cm.

Fig. 2. The right musk gland composes of round, polygonal or spindle neoplastic cells arranged in a diffuse pattern. In the parenchyma adjacent to the neoplastic tissue, papillary and cystic hyperplasia of luminal cells are noted. HE. Bar=100 μm.

Fig. 3. The neoplastic cells have hypochromatic nuclei and abundant cytoplasm with glassy eosinophilic inclusion (arrows). HE. Bar=10 μm.

Fig. 4. Papillary and cystic hyperplasia of luminal cells in the right musk gland. HE. Bar=20 μm.

Fig. 5. Metastatic foci of neoplastic rhabdoid cells in the lung. HE. Bar=20 μm.

Fig. 6. Neoplastic rhabdoid cells are positive for CK AE1/AE3 in the right musk gland. Immunohistochemistry. Bar=10 μm.

Fig. 7. Neoplastic rhabdoid cells are positive for GFAP in the right musk gland. Immunohistochemistry. Bar=10 μm.

Fig. 8. The cytoplasm of neoplastic rhabdoid cells contains whorl aggregates of intermediate filaments. TEM. Bar=1 μm.

Malignant rhabdoid tumors need to be distinguished diagnostically from other types of tumors such as histiocytic sarcoma, rhabdomyosarcoma, anaplastic carcinoma and fibrosarcoma. In the present case, the tumor exhibited positive staining for cytokeratins, vimentin, NSE and GFAP. Histiocytic/monocytic markers, such as CD204, HLA-DR, Iba-1 and lysozyme, are useful for diagnosing histiocytic sarcoma in domestic animals [5, 9, 24, 25]. Rhabdomyosarcoma is characterized by the expression of vimetin and desmin and detection of cross-striations by histopathological examinations [2]. Therefore, histiocytic sarcoma and

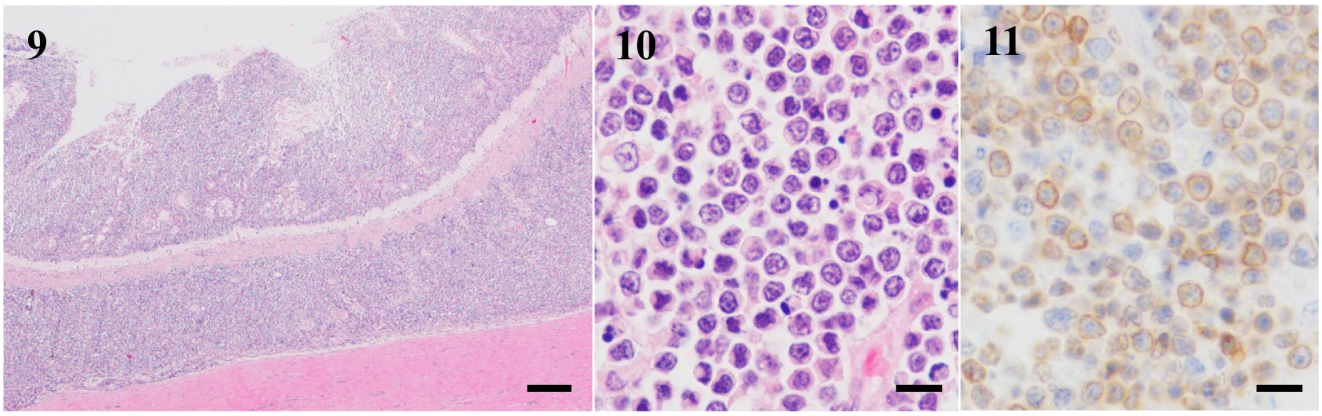

Fig. 9. Neoplastic lymphoid cells proliferate in the mucosal lamina propria and submucosa of the ileojejunam. HE. Bar=200 μm.

Fig. 10. Neoplastic lymphoid cells have a hypochromatic nucleus with large nucleoli and scarce cytoplasm. Higher magnification of Fig. 9. HE. Bar=10 μm.

Fig. 11. Neoplastic lymphoid cells are positive for CD3 in the mesenteric lymph node. Immunohistochemistry. Bar=10 μm.

rhabdomyosarcoma can be ruled out based on that the present neoplastic cells were negative for CD204, HLA-DR, Iba-1, lysozyme and desmin. Anaplastic carcinoma exhibits co-expression of cytokeratins and vimentin, however, the expression of GFAP and NSE as seen in the present case have not been reported [16].

The histogenesis of rhabdoid tumors is controversial because they express a variety of specific markers, including cytokeratins such as CK AE1/AE3, CK8 and CK18 and epithelial membrane antigen (EMA) for epithelial cells; vimentin for mesenchymal cells; αSMA and desmin for muscular cells; NSE, S-100, neurofilament and GFAP for neuroectodermal cells; and lysozyme and HLA-DR for histiocytes [3, 17, 19, 27]. In the 1980s, Neural crest or histiocytic lineage was suspected to be the cellular origin of these tumors [6, 7, 18]. Ota *et al*. (1993) reported that rhabdoid tumors are derived from primitive pluripotent cells that have the potential for a wide range of differentiation. In cats, the tumors arising from the skin are positive for vimentin, S-100, neurofilament and GFAP, indicating a neuroectodermal origin [10]. Besides rhabdoid tumors, rhabdoid features have previously been observed in a variety of malignant neoplasms, including malignant peripheral nerve sheath tumor, gastric adenocarcinoma and thyroid carcinoma [12, 17, 22].

To the best of our knowledge, this is the first report of malignant rhabdoid tumor and adenoma arising from the musk glands and systemic T-cell lymphoma in masked palm civet. Systemic T-cell lymphoma was considered as the cause of death in the present case.

REFERENCES

1. Beckwith, J. B. and Palmer, N. F. 1978. Histopathology and prognosis of Wilms tumor results from the first national Wilms' tumor study. *Cancer* **41**: 1937–1948. [Medline] [CrossRef]
2. Caserto, B. G. 2013. A comparative review of canine and human rhabdomyosarcoma with emphasis on classification and pathogenesis. *Vet. Pathol.* **50**: 806–826. [Medline] [CrossRef]
3. D'Antonio, A., Orabona, P., Caleo, A., Addesso, M., Liguori, G. and Boscaino, A. 2010. Primary rhabdoid tumor of thyroid gland. Description of a rare entity with molecular study. *Pathol. Int.* **60**: 644–646. [Medline] [CrossRef]
4. Ewer, R. F. 1973. The Carnivores. Cornell University Press, Ithaca.
5. Friedrichs, K. R. and Young, K. M. 2008. Histiocytic sarcoma of macrophage origin in a cat: case report with a literature review of feline histiocytic malignancies and comparison with canine hemophagocytic histiocytic sarcoma. *Vet. Clin. Pathol.* **37**: 121–128. [Medline] [CrossRef]
6. Gonzalez-Crussi, F., Goldschmidt, R. A., Hsueh, W. and Trujillo, Y. P. 1982. Infantile sarcoma with intracytoplasmic filamentous inclusions: distinctive tumor of possible histiocytic origin. *Cancer* **49**: 2365–2375. [Medline] [CrossRef]
7. Haas, J. E., Palmer, N. F., Weinberg, A. G. and Beckwith, J. B. 1981. Ultrastructure of malignant rhabdoid tumor of the kidney. A distinctive renal tumor of children. *Hum. Pathol.* **12**: 646–657. [Medline] [CrossRef]
8. Hong, C. B., Van Meter, P. W. and Latimer, C. L. 1999. Malignant rhabdoid tumour in the orbit of a horse. *J. Comp. Pathol.* **121**: 197–201. [Medline] [CrossRef]
9. Ishimori, M., Michishita, M., Yoshimura, H., Azakami, D., Ochiai, K., Ishiwata, T. and Takahashi, K. 2017. Disseminated histiocytic sarcoma with hemophagocytosis in a rabbit. *J. Vet. Med. Sci.* **79**: 1503–1506. [Medline] [CrossRef]
10. Izawa, T., Yamate, J., Takeda, S., Kumagai, D. and Kuwamura, M. 2008. Cutaneous rhabdoid tumor in a cat. *Vet. Pathol.* **45**: 897–900. [Medline] [CrossRef]
11. Lee, K., Iwata, T., Nakadai, A., Kato, T., Hayama, S., Taniguchi, T. and Hayashidani, H. 2011. Prevalence of *Salmonella, Yersinia* and *Campylobacter* spp. in feral raccoons (*Procyon lotor*) and masked palm civets (*Paguma larvata*) in Japan. *Zoonoses Public Health* **58**: 424–431. [Medline] [CrossRef]

12. Lu, Y. T., Huang, H. I., Yang, A. H. and Tai, S. K. 2016. Thyroid carcinoma with rhabdoid phenotype: Case report with review of the literature. *Auris Nasus Larynx* **43**: 706–709. [Medline] [CrossRef]
13. Machida, N., Izumisawa, N., Nakamura, T. and Kiryu, K. 1992. Canine distemper virus infection in a masked palm civet (*Paguma larvata*). *J. Comp. Pathol.* **107**: 439–443. [Medline] [CrossRef]
14. Malhotra, Y., Fitzgerald, T. N., Jubinsky, P. T., Harper, H., Silva, C. T., Zambrano, E., Diefenbach, K. A., Moss, R. L. and Bhandari, V. 2011. A unique case of rhabdoid tumor presenting as hemoperitoneum in an infant. *J. Pediatr. Surg.* **46**: 247–251. [Medline] [CrossRef]
15. Masuda, R., Lin, L. K., Pei, K. J., Chen, Y. J., Chang, S. W., Kaneko, Y., Yamazaki, K., Anezaki, T., Yachimori, S. and Oshida, T. 2010. Origins and founder effects on the Japanese masked palm civet Paguma larvata (Viverridae, Carnivora), revealed from a comparison with its molecular phylogeography in Taiwan. *Zool. Sci.* **27**: 499–505. [Medline] [CrossRef]
16. Misdorp, W., Else, R. W., Hellmen, E. and Lipscomb, T. P. 1999. Histological Classification of Mammary Tumors in the Dog and the Cat. 2nd ser. Vol. VII. Armed Forces Institute of Pathology, Washinton D. C.
17. Oda, Y. and Tsuneyoshi, M. 2006. Extrarenal rhabdoid tumors of soft tissue: clinicopathological and molecular genetic review and distinction from other soft-tissue sarcomas with rhabdoid features. *Pathol. Int.* **56**: 287–295. [Medline] [CrossRef]
18. Ota, S., Crabbe, D. C., Tran, T. N., Triche, T. J. and Shimada, H. 1993. Malignant rhabdoid tumor. A study with two established cell lines. *Cancer* **71**: 2862–2872. [Medline] [CrossRef]
19. Petitt, M., Doeden, K., Harris, A. and Bocklage, T. 2005. Cutaneous extrarenal rhabdoid tumor with myogenic differentiation. *J. Cutan. Pathol.* **32**: 690–695. [Medline] [CrossRef]
20. Rowlatt, U. 1967. Spontaneous epithelial tumours of the pancreas of mammals. *Br. J. Cancer* **21**: 82–107. [Medline] [CrossRef]
21. Schauer, G., Moll, R., Walter, J. H., Rumpelt, H. J. and Göltenboth, R. 1994. Malignant rhabdoid tumor in the gastric wall of an aged orangutan (*Pongo pygmaeus*). *Vet. Pathol.* **31**: 510–517. [Medline] [CrossRef]
22. Shomori, K., Sugamura, K., Adachi, K., Shiomi, T., Nanba, E. and Ito, H. 2011. Gastric adenocarcinoma with rhabdoid morphology. *Gastric Cancer* **14**: 290–294. [Medline] [CrossRef]
23. Steele, K. E., Schulman, F. Y., Mena, H. and Strimple, E. O. 1997. Rhabdoid tumor in the brain of a dog. *Vet. Pathol.* **34**: 359–363. [Medline] [CrossRef]
24. Thongtharb, A., Uchida, K., Chambers, J. K., Kagawa, Y. and Nakayama, H. 2016. Histological and immunohistochemical studies on primary intracranial canine histiocytic sarcomas. *J. Vet. Med. Sci.* **78**: 593–599. [Medline] [CrossRef]
25. Thongtharb, A., Uchida, K., Chambers, J. K., Miwa, Y., Murata, Y. and Nakayama, H. 2016. Histological and immunohistochemical features of histiocytic sarcoma in four domestic ferrets (Mustela putorius furo). *J. Vet. Diagn. Invest.* **28**: 165–170. [Medline] [CrossRef]
26. Wadsworth, P. F., Jones, D. M. and Pugsley, S. L. 1982. Primary hepatic neoplasia in some captive wild mammals. *J. Zoo An. Med.* **13**: 29–32. [CrossRef]
27. Weeks, D. A., Beckwith, J. B., Mierau, G. W. and Luckey, D. W. 1989. Rhabdoid tumor of kidney. A report of 111 cases from the national wilms' tumor study pathology center. *Am. J. Surg. Pathol.* **13**: 439–458. [Medline] [CrossRef]
28. Yonemitsu, K., Terada, Y., Kuwata, R., Nguyen, D., Shiranaga, N., Tono, S., Matsukane, T., Yokoyama, M., Suzuki, K., Shimoda, H., Takano, A., Muto, M. and Maeda, K. 2016. Simple and specific method for detection of antibodies against hepatitis E virus in mammalian species. *J. Virol. Methods* **238**: 56–61. [Medline] [CrossRef]